DOI: 10.1002/cphc.200((will be filled in by the editorial staff))

Pi Tetrel Bonds, and their Influence on Hydrogen Bonds and Proton Transfers

Yuanxin Wei, Qingzhong Li[1,*], Steve Scheiner[2,*]

((Dedication, optional))

The positive region that lies above the plane of F_2TO (T=C and Si) interacts with malonaldehyde (MDA) which contains an intramolecular H-bond. The T atom of F_2TO can lie either in the MDA molecular plane, forming a T···O tetrel bond, or F_2TO can stack directly above MDA in a parallel arrangement. The former structure is more stable than the latter, and in either case, F_2SiO engages in a much stronger interaction than does F_2CO, reaching up to nearly 200 kJ/mol. The π-tetrel bond strengthens/weakens the MDA H-bond when the bond is formed to the hydroxyl/carbonyl group of MDA, and causes an accompanying inhibition/promotion of proton transfer within this H-bond; this effect is stronger for F_2SiO. These same aspects can be tuned by substituents placed on any of the C atoms of MDA, although their effects are not fully correlated with the electron-withdrawing or releasing properties of the substituent. A new sort of π-π tetrel bond occurs when the π-hole on the T atom of F_2TO approaches the middle carbon atom of MDA from above, and a similar configuration is also found between F_2TO and benzene.

1. Introduction

Since it participates extensively in H-bonding and tunneling, two very important phenomena in chemical and biological systems,[1-5] the literature is replete with investigations of proton transfer.[1-10] The proton is often used as a promoter and mediator in chemical reactions.[3] Also, the proton can transfer into and out of proteins, which is important both for many enzyme reaction mechanisms and proton pumping across membranes.[6] Proton transfer reaction can be regulated by solvent polarity.[7,8] For example, pyrrole-2-carboxyldehyde undergoes excited state intramolecular proton transfer in hydrocarbon solvent but intermolecular proton transfer in hydroxylic polar solvent.[7]

Proton transfers are typically closely related to the strength of the H-bond in which they are involved, which can be enhanced or weakened by substituent[11] and cooperative effects.[12-21] An intramolecular H-bond was observed, for example, in 2-aminoethanol by infrared spectroscopy and non-covalent interaction analysis and it becomes stronger when electron-withdrawing groups adjoin with the OH carbon.[11] It was demonstrated that cooperative effects can occur between a H-bond and other types of noncovalent interactions,[12-21] among which the beryllium bond has a prominent effect, and leads to proton transfer.[12] However, Be-containing molecules are highly toxic, so complicate its use to regulate proton transfer in experimental situations. It was known that the low-barrier hydrogen bond (LBHB)[22-24] is favorable for proton transfer and plays an important role in enzymatic catalysis[23] and crystallography.[24]

The tetrel bond refers to an intermolecular interaction between a Group IV atom and an electron donor, and has witnessed rapidly expanding recent study. It has properties akin to hydrogen and halogen bonds in crystal materials,[25-27] chemical reactions,[28,29] and molecular recognition,[30,31] amongst many others.[32-39] As in H-bonds and related noncovalent interactions, the electron donors in tetrel bonds are also drawn from lone-pairs, π systems,[40] metal hydrides,[41] radicals,[42] and carbenes.[43,44] In addition, the tetrel bond exhibits cooperative effects with other interactions.[45-52] For instance, the tetrel and hydrogen bonds show positive cooperativity in F_2TO···NCH···NCH (T = C and Si), although two tetrel bonds interact negatively in HCN···F_2TO···NCH.[45] In contrast to numerous similarities, the tetrel bond can behave differently than the halogen bond in certain respects. As an example, the tetrel bond strengthens as the tetrel atom grows larger if it combines with a weak electron donor.[42] However, it becomes stronger in a different order: C < Ge < Sn < Si, when N-heterocyclic carbenes act as electron donors.[43] Importantly, F_2SiO can form a strong tetrel bond with strength comparable to a beryllium bond.[48] At this juncture, the mutual effects of a tetrel bond with an intramolecular H-bond have seen little examination.

As another issue, most tetrel bonds to this point are of the σ-type, wherein the electron donor approaches directly opposite one of the covalent bonds of the tetrel atom. There are relatively less known π-arrangements where the donor is situated above the plane of the tetrel-containing molecule. There has been even

[a] *Dr. Y. Wei, Q. Li*
Laboratory of Theoretical and Computational Chemistry and School of Chemistry and Chemical Engineering, Yantai University
Yantai 264005(China)
Fax: (+86)535-6902063
E-mail: cjb1962@vip.sina.com and li70316@sohu.com
[b] *Dr. Y. Wei, Q. Li*
Department of Chemistry and Biochemistry, Utah State University, Logan, UT 84322-0300 (USA)
E-mail: steve.scheiner@usu.com

*Supporting information for this article is available on the WWW under http://www.chemphyschem.org or from the author.((**Please delete if not appropriate**))*

less study of the case where the two planar molecules are stacked above one another so as to form a tetrel bond, although this is a common arrangement in the general case.[53-55] For example, Zhao and Zhang performed an energy decomposition analysis for the π-π stacking in benzene dimer and found that orbital interaction provides additional considerable contribution besides electrostatic and dispersion energies.[55] There appears to be a distance dependence of substituent effects on parallel π-π stacking interactions,[56] which is in agreement with the Hunter–Sanders model.[57] A combination of π-π stacking and other interactions might be utilized to prepare self-assembled nanostructures[58] and to capture carbon dioxide.[59] However, π-π stacking involving F_2TO (T=tetrel), with its potential tetrel bond, has not to our knowledge been studied thus far.

In the present study, malonaldehyde (MDA) was taken as a prototypical molecule containing an internal H-bond, with the potential of proton transfer within. MDA is a product of polyunsaturated fatty acid peroxidation, usually regarded as a marker of oxidative stress and antioxidant status in cancer cells.[60,61] MDA is mainly used as a pharmaceutical intermediate and a raw material for photosensitive pigments. Thus its structures and properties have been investigated and received additional consideration.[60-66] MDA was allowed to interact with F_2TO (T=C and Si) so as to examine the nature of any tetrel bonds that might be formed, and how such interactions might influence the internal H-bond and proton transfer. It is notable that any tetrel bonds that might be formed by F_2TO would involve the positive region above the plane of this molecule, a so-called π-hole, rather than the more typical σ-hole which by definition is located directly opposite a T-R covalent bond. When interacting with MDA, the F_2TO can lie in the plane of MDA or can stack directly above it in a parallel arrangement. These two geometries, with very different sorts of bonding, and with potentially very different effects upon the internal H-bond of MDA, can thus be directly compared with one another. By examining both F_2CO and F_2SiO, it is possible to extract information about how the C and Si atoms compare with one another in this context. One can also derive insights about the relative strengths and properties of tetrel bonds vs the H-bonds that can occur between MDA and F_2TO, and how these two types of interactions might affect one another. As an additional issue, various substituents were placed on MDA, in different positions, so as to further influence the tetrel bond and its capability to influence the proton transfer process.

2. Theoretical Methods

Monomers, dimer, and trimers were optimized at the MP2 level in the framework of the aug-cc-pVTZ basis set. Frequency calculations were carried out at the same level to verify that the optimized structures are true minima on the potential energy surface. Interaction energies were calculated using the supermolecular approach, in which the monomer geometries in the complexes were used, and corrected for the basis set superposition error (BSSE) using the counterpoise method of Boys and Bernardi.[67] All calculations were performed with the Gaussian09 program.[68]

Molecular electrostatic potentials (MEPs) on the 0.001 au isodensity surface were calculated at the MP2/aug-cc-pVDZ level using the wave function analysis−surface analysis suite (WFA-SAS) program.[69] Topological analyses were performed using the atoms in molecules (AIM) methodology at the MP2/aug-cc-pVDZ level. AIM 2000 software[70] was used to calculate electron densities, Laplacians, and energy densities at bond critical points. The second-order perturbation energy was obtained at the HF/aug-cc-pVTZ level via the natural bond orbital (NBO) method[71] implemented in Gaussian09. Interaction energies were decomposed using the LMOEDA method[72] at the same level by the GAMESS program.[73] Non-covalent interaction (NCI) analysis was performed using the Multiwfn program[74] and the related plots were graphed using the VMD program.[75]

3. Results and Discussion

3.1. Coplanar Tetrel-Bonded Complexes

Malondialdehyde (MDA), which is often taken as a model to study intramolecular proton transfer,[12] exists mainly in its enol form and the cis-isomer is favored in organic solvents. F_2TO (T =C and Si) was added to MDA to examine the nature of the interaction, and how it might affect this transfer. By its nature, F_2TO contains several sites that can act as either electron donor or acceptor with MDA. The electrostatic potential surrounding MDA is exhibited in Figure 1, where negative (blue) regions surround the two O atoms. These atoms are thus prime candidates to engage in a tetrel bond with the positive π-hole on the T atom of F_2TO. The latter appears as the red region above the T atoms of F_2CO and F_2SiO in Figure 1. The values of the maxima are rather large, 219.8 for F_2CO and twice as large in its Si analogue, so these are indeed prime candidates for formation of tetrel bonds. And in fact, such tetrel-bonded structures represent minima on the potential energy surface, as shown in Figure 2, which also contains the interaction energy of each complex in parentheses. Owing to the positive (red) areas that surround the CH protons of MDA, they are capable of engaging in CH···O H-bonds with the O atoms of F_2TO. Those geometries in which such H-bonds, generally bifurcated, are the primary feature are displayed in Figure S1.

The π-hole on the T atom of F_2TO may interact with either the hydroxyl or carbonyl O atom of MDA, designated by the a and b labels, respectively. Moreover, the CH of MDA may approach either the O or an F atom of F_2TO, designated respectively as 1 and 2. The H-bonds in the former mode are generally shorter, 2.226-2.531 Å vs 2.706-3.163 Å for the latter. In fact, the characterization of these CH···F interactions as a true H-bond is dubious, as witness the absence of a corresponding BCP in Figure S2.

As Figure 1 confirms the more negative potential on the carbonyl vs the hydroxyl O of MDA, it is not surprising that the former forms a stronger tetrel bond with F_2TO than does the latter. This differential is reflected by the shorter C···O distances, the more negative interaction energy, and the larger electron density at the C···O BCP in the C-b complexes. The importance of electrostatic energy to the relative stabilities of TB-C-a and TB-C-b is also confirmed by the energy decomposition which is contained in Table 1. Replacement of C by Si removes the minima where the F_2SiO approaches the hydroxyl O of MDA, leaving only TB-Si-a-1 and TB-Si-a-2. The former is more stable in part due to the presence of the CH···O H-bond.

In terms of interaction energies, the Si complexes are many times stronger than their C-analogues. While the latter is in the 13-22 kJ/mol range, those involving Si approach 200 kJ/mol. Some insights into the relative stabilities of these minima can be gleaned from the energy components in Table 1. In all cases, the electrostatic and exchange energies are similar in magnitude, with the latter slightly larger. Polarization energy is smaller, especially for the C series, where it is comparable to the dispersion attraction. All of these terms are very substantially

magnified for the Si complexes. It is interesting that the decomposition scheme provides positive dispersion energy for the latter pair, a counterintuitive result. This is due to the differences in the intra- and intermolecular correlation energy on going from noninteracting to interacting molecules.[73]

The formation of these complexes has a significant effect upon the intramolecular structure of MDA, and in particular its internal H-bond. r(OH) is stretched a small amount when the C-tetrel bond is formed with the hydroxyl O, and the R(H···O) H-bond shortened. These changes can be described as a partial proton transfer. The opposite perturbations, characteristic of a less transferred proton, occur when the tetrel bond involves the carbonyl O, whether F_2CO or F_2SiO, although these effects are magnified for the latter. It was earlier observed that BeF_2 also promotes the proton transfer in MDA.[12]

3.2. π-π Parallel Structures

A face-to-face parallel π-π structure emerges when the π-hole on the T atom of F_2TO approaches the central carbon atom of MDA from above, much like π-π interactions in aromatic systems.[54-56] There have been no prior reports of these sorts of tetrel bonds, diagrammed at the bottom of Figure 2, to our knowledge. As in the case of the coplanar geometries, F_2SiO forms a much stronger π-π tetrel bond than does F_2CO, by a factor of 11. Indeed, the interaction energy in TB-Si-c of -113.0 kJ/mol is quite a bit larger than those in stacked π-π aromatic systems.[55] On the other hand, these π tetrel bonds are a bit weaker than their coplanar analogues, roughly 50-60%. The bulk of this relative weakness derives from a diminution of the electrostatic attraction, as revealed by Table 1. This distinction is not surprising in view of the near absence of a negative region above the plane of the MDA molecule in Figure 1, with which the F_2TO π-hole can interact. The large dispersion energy in TB-C-c is similar to that in π-π interactions in aromatic systems.[55]

With regard to how these sorts of interactions might affect the intramolecular HB of MDA, the geometric aspects of TB-C-c are virtually unchanged from the monomer. In the Si analogue, however, there is a certain degree of proton transfer, with r(OH) stretching by some 0.02 Å, and a 0.07 Å reduction of the R(H···O) distance.

As indicated above, the high positive charge on the CH protons is favorable for formation of coplanar fully H-bonded structures, illustrated in Figure S1. The most positive of these is associated with the CH closest to the -OH group, which helps explain the greater stability of HB-C-a and HB-Si-a vs HB-C-b and HB-Si-b. It might also be noted that F_2SiO engages in stronger HBs than does F_2CO, consistent with the lesser electronegativity of Si. Nevertheless, these H-bonded Si complexes are far less stable than the tetrel-bonded dimers; the same is true in the C-analogues, but the margin is much smaller.

It is instructive to compare the π-π tetrel bonds formed by F_2TO with MDA and with benzene. It is apparent from Figure 3 that whereas benzene forms a stronger stacked complex with F_2CO than does MDA, the reverse is true for F_2SiO which is much more strongly attracted to MDA than to benzene. With regard to energy components, Table 1 shows that they are quite similar for F_2CO/MDA and F_2CO/benzene, except for a bit more dispersion attraction in the latter, which accounts for its greater stability. Their stability arises from nearly equal measures of electrostatic and dispersion forces. The Si analogues show a much greater discrepancy between MDA and benzene, with all components larger for the former. The largest component appears to be polarization, followed closely by electrostatics.

There is the question of categorizing the interaction in this parallel orientation. Would it be best termed a stacked π-π interaction as might occur for example in benzene dimer, or is it better described as a tetrel bond? In the case of F_2CO, the electrostatic term is slightly exceeded by dispersion, both of which dwarf the polarization energy. The large contribution of dispersion might suggest a π-π stacking attraction. The situation is quite different for F_2SiO, however, where dispersion attraction is quite small, and electrostatics and polarization are very large contributors. The latter distribution is consistent with tetrel and similar sorts of bonds. In terms of geometry the Si atom is situated almost directly above a C atom of MDA or benzene, rather than over the center of the molecule as a whole, another indicator that the interaction is not of standard π-π type. Note from Figure 1 that the most negative point above the MDA molecule is displaced away from the central C atom, closer to the OH, so the placement of the F_2SiO is not dictated purely by electrostatic issues.

Another perspective may be gleaned from NCI analysis of these complexes. As may be noted from Figure S3, all of the parallel structures contain a green region between them, indicative of a certain degree of noncovalent bonding. On the other hand, it is difficult to pin down which pairs of atoms are directly interacting with one another due to the diffuse nature of this green bonding area. A better means to examine the latter question arises from AIM analysis of the electron densities. Figure S2 shows that the stacked complexes do indeed contain a bond path between the two molecules. The density at the bond critical point is rather small for the F_2CO complex TB-C-c, 0.009 au. Moreover, the path does not terminate on the C atom of F_2CO, but rather on the C=O bond, closer to the O. In the Si analogue however, the path unambiguously connects Si to the central C atom of MDA, with a larger magnitude of ρ_{BCP}=0.064, and thus constitutes much clearer evidence of a tetrel bond. Very similar trends are apparent in the benzene analogues pictured in Figure S4, where the tetrel bond is much clearer in evidence for F_2SiO than for F_2CO.

BZ-C-a and BZ-C-b differ by the orientation of the F_2CO, similar to BZ-Si-a and BZ-Si-b. The energetics are not very sensitive to this rotation. In a related observation for the benzene homodimer, the interaction energies for the sandwich and parallel-displaced configurations are estimated to be 1.8 (2.0) and 2.8 (2.7) kcal/mol, respectively.[76] It is found that π-π tetrel bond and π-π stacking are comparable in strength and even the former is a little stronger than the latter. Based on the importance of π-π stacking in crystal materials,[77] it is deduced that π-π tetrel bond is also important in crystal materials.

3.3. Dimer of the Keto Tautomer

As the keto form of MDA is energetically viable, its complexes with F_2TO were also examined. As may be seen in Figure S5, there are three main interaction modes. A tetrel bond is complemented by a CH···O interaction to one of the two CHO groups of MDA in modes d and e which are quite similar to one another. The same sorts of interactions occur in mode f, except that the CH···O H-bond involves the central CH_2 group. The interaction energies of d and e are 20.2 kJ/mol for T=C, and much larger, roughly 160 kJ/mol for T=Si. These quantities are comparable to those for the enol tautomer.

A weak internal CH···O interaction is present in the keto form of MDA monomer, which is confirmed by a low and narrow spike in Figure S6. In the complexes with F_2CO, the tetrel bond makes the CH···O separation in MDA longer for each interaction mode.

A similar effect is observed in the e mode of F_2SiO although its effect is larger than that of F_2CO. However, the CH···O separation in MDA is shorter in the d and f modes of F_2SiO, and is 2.479 Å in TB-Si-f, which is well below the sum of the respective vdW radii (~3.3 Å). Even so, the position of the spike corresponding to the CH···O interaction is not shifted greatly (Figure S6) and thus the strength of the CH···O interaction undergoes a small enhancement in TB-Si-f.

3.4. Effects of Substituents on Intramolecular Hydrogen Bond

In addition to external influences, the intramolecular HB of MDA can also be tuned by the presence of substituents. Moreover, these substituents can be placed either on the central C_2 atom or one of the other two (C_1 and C_3). The nitro group (NO_2) was chosen as a highly electron-withdrawing substituent and NH_2 as its opposite. Each of these substituents was placed on C_1, C_2, and C_3, as illustrated in Figure 4, and the geometry fully optimized. Black numbers in Figure 4 refer to the electron density at the H···O bond critical point, while atomic charges are indicated in blue. The second-order perturbation energy due to the $LP_O \rightarrow \sigma^*_{O-H}$ orbital interaction in MDA and its derivatives is given in Table 2. These energies are relatively large and the largest energy is 392.1 kJ/mol in 1-NH_2-MDA. This is mainly attributed to the strong and short intramolecular H-bond in these molecules, evidenced by the shortest H···O distance (1.432 Å) in 1-NH_2-MDA.

Considering the nitro group first, as it transitions from C_1 to C_2 to C_3, ρ_{BCP} undergoes considerable reduction, suggesting a progressive weakening of the H-bond. In other words, the electron-withdrawal strengthens the proton-donating ability of the neighboring OH group in the C_1 position, but weakens the proton-accepting power of the carbonyl O when NO_2 is situated more closely to it in the C_3 position. This same idea explains the lowering positive partial charge on the bridging proton as the nitro group moves from site to site. This pattern is repeated in the NBO $LP_O \rightarrow \sigma^*_{O-H}$ values of $E^{(2)}$ in Table 2, which also shows a weakening of the H-bond as the NO_2 group moves from left to right. These trends are consistent with general ideas of H-bonding.

In the case of NH_2, however, its presence near the OH group strengthens the H-bond, and also makes the H more positive, in spite of the amino group's electron-releasing functionality. This H-bond enhancement is also reflected in the very large $E^{(2)}$ for 1-NH_2-MDA in Table 2. The motion of this substituent to C_2 and C_3 weakens the H-bond, but there is little difference between the latter two positions. The combined placement of NO_2 on C_1 and NH_2 on C_3 yields a large value of $E^{(2)}$, although still less than that of 1-NH_2-MDA, which represents a bit of an anomaly.

According to the above analysis of the charge, it is found that its change is sometimes not in agreement with the change of the hydrogen bonding strength. For example, an increase is found for the negative charge on the oxygen atom of the aldehyde group and the positive charge on the hydrogen atom of the hydroxyl group in 3-NH_2-MDA. However, the corresponding hydrogen bond is weakened. When the hydrogen atoms in C_1-H and C_3-H are replaced by NO_2 and NH_2, respectively, both the negative charge on the oxygen atom of the aldehyde group and the positive charge on the hydrogen atom of the hydroxyl group will increase with respect to those in 1-NO_2-MDA. However, the hydrogen bond is weaker in 1-NO_2-3-NH_2-MDA than in 1-NO_2-MDA. Consequently, we think that the substituent effect in MDA is not mainly realized through electrostatic interaction.

As indicated in Figure 4, when a benzene ring is fused with MDA, both the negative charge on the oxygen atom of the aldehyde group and the positive charge on the hydrogen atom of the hydroxyl group decrease due to the delocalization of the benzene ring. Its effect is similar to NO_2 in 3-NO_2-MDA, resulting in a weakening of the H-bond, as noted in the last row of Table 2.

Based on the second-order perturbation energies listed in Table 2, it is interesting to compare the effect of substituents and additional tetrel bonds on the strength of the intramolecular H-bond in MDA. When F_2CO is added to the hydroxyl O atom, its effect is equivalent to that of NO_2 in C_2, while it exhibits the similar effect to the NH_2 in C_2 if it binds with the carbonyl O atom. The π-π tetrel bond in TB-C-c and TB-Si-C leads to the similar enhancement for the intramolecular H-bond with 3-NH2-MDA and 1-NO2-MDA, respectively. The second-order perturbation energies in TB-Si-a-1 and TB-Si-a-2 have a prominent decrease, providing a further evidence for the proton transfer in both complexes.

3.5. CSD research

It would be very instructive to search for supporting structural information from accurately determined molecular structures deposited in the CSD (Cambridge Structural Database). To obtain experimental evidence for the π···π interactions between two C atoms, we performed a survey of the CSD. Based on the van der Waals radius of C (1.70 Å)[78] and its covalent radius (0.75 Å)[79], the criteria for the intermolecular distances were chosen as 1.50-3.40 Å for C···C between carbonyl group and benzene derivatives. More than 300 relevant structures are found and a pair of representative crystal structures is displayed in Figure 5. An almost perfectly parallel C···C π···π interaction is formed between two molecules in LAWZIP and BELKEJ. The binding distances are 3.196 and 3.195, 3.234 Å, respectively. This shows that the C···C π···π interaction is significant for stabilizing and maintaining crystal structures.

4. Conclusions

F_2CO and F_2SiO both contain a π-hole, a positive region directly above the central T atom. This π-hole prefers to interact with the O atoms of MDA, particularly the carbonyl O. The ensuing π-tetrel bond is much stronger for F_2SiO than for its C counterpart, approaching 200 kJ/mol. Electrostatic interaction plays a major role in this interaction. This interaction influences the strength of MDA's intramolecular H-bond, as well as the position of its bridging proton. In fact, the tetrel bond can even induce the proton to transfer from one O atom of MDA to the other. The F_2TO molecule can also adopt a position where in its T atom lies directly above the central C atom of MDA, forming a π···π tetrel bond. Again, this sort of bond is also much stronger for F_2SiO than for F_2CO. Whether a C···O or π···π configuration, the tetrel bond is dominated by equal contributions from electrostatics and dispersion for F_2CO, but dispersion is largely absent for F_2SiO where polarization is the major secondary contributor.

Substituents also affect the strength of MDA's intramolecular hydrogen bond, related to both the nature of the substituent and its position. Both an electron withdrawing (NO_2) and an electron-donating group (NH_2) strengthen the H-bond when adjacent to the hydroxyl group, while placement near the carbonyl group has the opposite effect. The former enhancing effect is more prominent for NH_2, while the latter weakening is greater for NO_2. When

substitution occurs at the middle carbon atom, NO_2 strengthens the bond while NH_2 weakens it.

Acknowledgements

This work was supported by the National Natural Science Foundation of China (21573188) and Graduate Innovation Foundation of Yantai University (YDYB1713).

Keywords: (Intramolecular proton transfer; π-π tetrel bond; Substituent effects)

[1] T. Gensch, J. Heberle, C. Viappiani, *Photochem. Photobiolog. Sci.* **2006**, *5*, 529–530.
[2] H. Matsuzawa, T. Nakagaki, M. Iwahashi, *J. Oleo Sci.* **2007**, *56*, 653–658.
[3] M. Eigen, *Angew. Chem. int. Ed.* **1964**, *3*, 1–19.
[4] A. Filarowski, A. Koll, P. E. Hansen, M. Kluba, *J. Phys. Chem. A* **2008**, *112*, 3478–3485.
[5] G. L. Vedat, D. O. Isin, *Chin. J. Struct. Chem.* **2014**, *33*, 1757–1767.
[6] S. J. Ferguson, *Curr. Biol.* **2000**, *10*, R627–R630.
[7] N. Muller, C. Reiter, *J. Chem. Phys.* **1965**, *42*, 3265–3269.
[8] S. Hu, K. Liu, Y. Z. Li, Q. Q. Ding, W. Peng, M. Chen, *Can. J. Chem.* **2013**, *92*, 274–278.
[9] A. A. M. Prabhu, S. Siva, R. K. Sankaranarayanan, N. Rajendiran, *J. Fluoresc*. **2010**, *20*, 43–54.
[10] F. A. S. Chipem, A. Malakar, G. Krishnamoorthy, *Photochem. Photobiol.* **2015**, *91*, 298–305.
[11] J. R. Lane, S. D. Schrøder, G. C. Saunders, H. G. Kjaergaard, *J. Phys. Chem. A* **2016**, *120*, 6371–6378.
[12] O. Mó, M. Yáñez, I. Alkorta, J. Elguero, *J. Chem. Theory Comput*. **2012**, *8*, 2293−2300
[13] Q. Z. Li, X. L. An, B. A. Gong, J. B. Cheng, *J. Phys. Chem. A* **2007**, *111*, 10166–10169.
[14] B. A. Gong, B. Jing, Q. Z. Li, Z. B. Liu, W. Z. Li, J. B. Cheng, Q, C. Zheng, J. Z. Sun, *Theor. Chem. Acc.* **2010**, *127*, 303–309.
[15] Q. Z. Li, Z. B. Liu, J. B. Cheng, W. Z. Li, B. A. Gong, J. Z. Sun, *J. Mol. Struct. Theochem*. **2009**, *896*, 112–115.
[16] T. Kar, S. Scheiner, *J. Phys. Chem. A* **2004**, *108*, 9161–9168.
[17] S. S. Xantheas, *Chem. Phys.* **2000**, *258*, 225–231.
[18] G. A. Jeffrey, An Introduction to Hydrogen Bonding.: Oxford university press. New York, **1997**.
[19] J. Ireta,; J. Neugebauer, M. Scheffler, A. Rojo, *J. Phys. Chem. B* **2003**, *107*, 1432–1437.
[20] N. Dominelli-Whiteley, J. J. Brown, K. B. Muchowska, I. K. Mati, C. Adam, T. A. Hubbard, A. Elmia, A. J. Brown, I. A. W. Bellb, S. L. Cockroft, *Angew. Chem. Int. Ed.* **2017**, *56*, 7658–7662.
[21] X. L. An, X. Yang, B. Xiao, J. B. Cheng, Q. Z. Li, *Mol. Phys.* **2017**, *115*, 1–10.
[22] H. ChojnackiInt, *J. Mol. Sci*. **2003**, *4*, 408-409.
[23] T. Graen, L. Inhester, M. Clemens, H. Grubmüller, G. Groenhof, *J. Am. Chem. Soc.* **2016**, *138*, 16620-16631.
[24] D. A. Nichols, J. C. Hargis, R. Sanishvili, P. Jaishankar, K. Defrees, E. W. Smith, K. K. Wang, F. Prati, A. R. Renslo, H. L. Woodcock, Y. Chen, *J. Am. Chem. Soc.* **2015**, *137*, 8086-8095.
[25] A. Bauzá, T. J. Mooibroek, A. Frontera, *Chem. Int. Ed.* **2013**, *52*, 12317–12321.
[26] A. Bauzá, T. J. Mooibroek, A. Frontera, *Chem. Commun*. **2014**, *50*, 12626–12629.
[27] M. S. Gargari, V. Stilinović, A. Bauzá, A. Frontera, P. McArdle, D. V. Derveer, S. W. Ng, G. Mahmoudi, *Chem. Eur. J.* **2015**, *21*, 17951–17958.
[28] S. J Grabowski, *Phys. Chem. Chem. Phys*. **2014**, **16**, 1824–1834.
[29] M. X. Liu, Q. Z. Li, J. B. Cheng, W. Z. Li, H. B Li, *J. Chem. Phys.* **2016**, *145*, 224310.
[30] S. Scheiner, *J. Phys. Chem. A* **2017**, *121*, 3606−3615.
[31] S. Scheiner, *Chem. Eur. J.* **2016**, *22*, 18850−18858.
[32] D. Mani, E. Arunan, *Phys. Chem. Chem. Phys*. **2013**, *15*, 14377–14383.
[33] S. P. Thomas, M. S. Pavan, T. N. G. Row, *Chem. Commun*. **2014**, *50*, 49–51.
[34] S. Scheiner, *J. Phys. Chem. A* **2015**, *119*, 9189−9199.
[35] A. Bauzá, T. J. Mooibroek, A. Frontera, *Chem. Rec.* **2016**, *16*, 473–487.
[36] V. P. Nziko, S. Scheiner, *Phys. Chem. Chem. Phys*. **2016**, *18*, 3581–3590.
[37] M. X. Liu, Q. Z. Li, W. Z. Li, J. B. Cheng , S. A. C. McDowell, *RSC Adv*. **2016**, *6*, 19136–19143.
[38] Q. C. Wei, Q. Z. Li, J. B. Cheng, W. Z. Li, H. B. Li, *RSC Adv*. **2016**, *6*, 79245–79253.
[39] M. X. Liu, Q. Z Li, S. Scheiner, *Phys. Chem. Chem. Phys*. **2017**, *19*, 5550–5559.
[40] D. Mani, E. Arunan, *J. Phys. Chem. A* **2014**, *118*, 10081−10089.
[41] Q. Z. Li, H. Y. Zhuo, H. B. Li, Z. B. Liu, W. Z. Li, J. B. Cheng, *J. Phys. Chem. A* **2015**, *119*, 2217−2224.
[42] Q. Z. Li, X. Guo, X. Yang, W. Z. Li, J. B. Cheng , H. B. Li, *Phys. Chem. Chem. Phys*. **2014**, *16*, 11617–11625.
[43] M. X. Liu, Q. Z. Li, W. Z. Li, J. B. Cheng, *Struct. Chem.* **2017**, *28*, 823–831
[44] J. E. Del Bene, I. Alkorta, J. Elguero, *J. Phys. Chem. A* **2017**, *121*, 4039−4047.
[45] Q. J. Tang, Q. Z. Li, *Comput. Theoret. Chem.* **2014**, *1050*, 51–57.
[46] X. Guo, Y. W. Liu, Q. Z. Li, W. Z. Li, J. B. Cheng, *Chem. Phys. Lett*. **2015**, *620*, 7–12.
[47] H. L. Xu, J. B. Cheng, X. Yang, Z. B Liu, B. Xiao, Q. Z. Li, *RSC Adv.* **2017**, *7*, 21713–21720.
[48] H. L. Xu, J. B. Cheng, X. Yang, Z. B Liu, B. Xiao, W. Z. Li, Q. Z. Li, *ChemPhysChem* **2017**, *18*, 2442–2450.
[49] S. Yourdkhani, T. Korona, N. L. Hadipour, *J. Comput. Chem*. **2015**, *36*, 2412–2428.
[50] M. Marín-Luna, I. Alkorta, J. Elguero, *J. Phys. Chem. A* **2016**, *120*, 648–656.
[51] W. Li, Y. L. Zeng, X. Y. Li, Z. Sun, L. P. Meng, *Phys. Chem. Chem. Phys.* **2016**, *18*, 24672–24680.
[52] X. Yang, P. P. Zhou, F. Yang, D. G. Zhou, C. X. Yan, P. J. Zheng, Y. Dai, *ChemistrySelect* **2016**, *1076*, 32–34.
[53] C. Trujillo, G. Sánchez-Sanz, *ChemPhysChem* **2016**, *17*, 395–405.
[54] N. J. Silva, F. B. C. Machado, H. Lischka, A. J. A. Aquino, *Phys. Chem. Chem. Phys.* **2016**, *18*, 22300–22310.
[55] R. D. Zhao, R. Q. A Zhang, *Phys. Chem. Chem. Phys*. **2016**, *18*, 25452–25457.
[56] L. J. Riwar, N. Trapp, B. Kuhn, F. Diederich, *Angew. Chem. Int. Ed*. **2017**, *56*, 11252–11257.
[57] C. A. Hunter, J. K. M. Sanders, *J. Am. Chem. Soc.* **1990**, *112*, 5525–5534.
[58] S. Y. L. Leung, S. Evariste, C. Lescop, M. Hissler, V. W. W. Yam, *Chem. Sci.* **2017**, *8*, 4264–4273.
[59] L. Yang, G. Chang, D. Wang, *ACS Appl. Mater. Inter.* **2017**, *9*, 15213−15218.
[60] S. Gaweł, M. Wardas, E. Niedworok, P. Wardas, *Wiad. Lek*. **2004**, **57**, 453–455.
[61] D. Del-Rio, A. J.Stewart, N. Pellegrini, *Nutr. Metab. Cardiovasc. Dis.* **2005**, *15*, 316–328.
[62] J. Huang, M. Buchowiecki, T. Nagy, J. Vaníček, M. Meuwly, *Phys. Chem. Chem. Phys.* **2014**, *16*, 204–211.
[63] Y. Wang, J. M. Bowman, *J. Chem. Phys*. **2013**, *139*, 154303.
[64] C. Trujillo, G. Sánchez-Sanz, I. Alkorta, J. Elguero, O. Mo, M. Yáñez, *J. Mol. Struct*. **2013**, *1048*, 138–151.
[65] K. R. Nandipati, H. Singh, R. S. Nagaprasad, K. A. Kumar, S. Mahapatra, *Eur. Phys. J. D* **2014**, *68*, 355–365.
[66] H. Kojima, A. Yamada, S. A Okazaki, *J. Chem. Phy*. **2015**, *142*, 174502.
[67] S. F. Boys, F. Bernardi, *Mol. Phys*. **1970**, *19*, 553–566.
[68] M. J. Frisch, G. W. Trucks, H. B. Schlegel, G. E. Scuseria, M. A. Robb, J. R. Cheeseman, G. Scalmani, V. Barone, B. Mennucci, G. A. Petersson, H. Nakatsuji, M. Caricato, X. Li, H. P. Hratchian, A. F. Izmaylov, J. Bloino, G. Zheng, J. L. Sonnenberg, M. Hada, M. Ehara, K. Toyota, R. Fukuda, J. Hasegawa, M. Ishida, T. Nakajima, Y. Honda, O. Kitao, H. Nakai, T. Vreven, J. J. A. Montgomery, J. E. Peralta, F. Ogliaro, M. Bearpark, J. J. Heyd, E. Brothers, K. N. Kudin, V. N. Staroverov, R. Kobayashi, J. Normand, K. Raghavachari, A. Rendell, J. C. Burant, S. S. Iyengar, J. Tomasi, M. Cossi, N. Rega, J. M. Millam, M. Klene, J. E. Knox, J. B. Cross, V. Bakken, C. Adamo, J. Jaramillo, R. Gomperts, R. E. Stratmann, O. A. Yazyev, J. Austin, R. Cammi, C. Pomelli, J. W. Ochterski, R. L. Martin, K. Morokuma, V. G. Zakrzewski, G. A. Voth, P. Salvador, J. J. Dannenberg, S. A. Dapprich, D. Daniels, O. Farkas, J. B. Foresman, J. V.

Ortiz, J. Cioslowski , D. J. Fox, Gaussian 09, Revision A.02, Gaussian, Inc. Wallingford, CT **2009**
[69] F. A. Bulat, A. Toro-Labbé, T. Brinck, J. S. Murray, P. Politzer, *J. Mol. Model*. **2010**, *16*, 1679–1691.
[70] R. F. W. Bader, AIM2000 Program, v. 2.0, McMaster University, Hamilton, Canada, **2000**.
[71] A. E. Reed, L. A. Curtiss, F. Weinhold, *Chem. Rev*. **1988**, *88*, 899–926.
[72] M. W. Schmidt, K. K. Baldridge, J. A. Boatz, S. T. Elbert, M. S. Gordon, J. H. Jensen, S. Koseki, N. Matsunaga, K. A. Nguyen, S. J. Su, T. L. Windus, M. Dupuis, J. A. Montgomery, *J. Comput. Chem*. **1993**, *14*, 1347–1363.
[73] P. F. Su, H. Li, *J. Chem. Phys*. **2009**, *13*, 014102.
[74] T. Lu , F. Chen, *J. Comput. Chem*. **2012**, *33*, 580–592.
[75] W. Humphrey, A. Dalke , K. Schulten, *J. Mol. Graphics* **1996**, *14*, 33–38.
[76] M. O. Sinnokrot, E. F. Valeev, C. D. Sherrill, *J. Am. Chem. Soc.* **2002**, *124*, 10887–10893.
[77] G. F. Liu, B. H. Ye, Y. H. Ling, X. M. Chen, *Chem. Commun*. **2002**, *0*, 1442–1443.
[78] A. Bondi, *J. Phys. Chem.* **1964**, *68*, 441–451.
[79] P. Pyykk¨o, M. Atsumi, *Chem. Eur. J*. **2009**, *15*, 186–197.

Received: ((will be filled in by the editorial staff))
Publ*ished onl***ine:** ((will be filled in by the editorial staff))

Table 1. Electrostatic (E^{ele}), exchange (E^{ex}), repulsion (E^{rep}), polarization (E^{pol}), and dispersion (E^{disp}) energies. All are in kJ/mol.

Complexes	E^{ele}	E^{ex}	E^{rep}	E^{pol}	E^{disp}
TB-C-a-1	-29.6	-34.1	61.0	-6.5	-7.9
TB-C-b-1	-43.7	-50.7	91.7	-11.45	-7.4
TB-C-a-2	-20.3	-25.6	46.4	-4.6	-8.4
TB-C-b-2	-31.3	-36.5	66.5	-7.6	-7.5
TB-C-c	-16.8	-35.2	63.5	-4.56	-17.3
BZ-C-a	-16.3	-41.2	71.8	-5.1	-23.6
BZ-C-b	-18.0	-37.1	65.7	-4.1	-20.6
TB-Si-a-1	-391.3	-396.8	825.5	-282.2	49.2
TB-Si-a-2	-348.9	-350.5	739.6	-266.2	46.7
TB-Si-c	-237.9	-351.2	723.6	-252.6	2.5
BZ-Si-a	-115.2	-232.0	448.3	-160.5	-22.0
BZ-Si-b	-121.5	-227.7	443.2	-151.9	-17.8

Table 2. Second-Order Perturbation Energy ($E^{(2)}$, kJ/mol) due to the $Lp_{O}\rightarrow\sigma^{*}_{O\text{-}H}$ Orbital Interaction.

Molecules	$E^{(2)}$	Molecules	$E^{(2)}$
MDA	148.9	---	---
TB-C-a-1	167.2	1-NO_2-MDA	210.8
TB-C-b-1	136.3	2-NO_2-MDA	162.6
TB-C-a-2	162.1	3-NO_2-MDA	81.0
TB-C-b-2	130.1	1-NH_2-MDA	392.1
TB-C-c	147.5	2-NH_2-MDA	137.5
TB-Si-a-1	62.1	3-NH_2-MDA	144.1
TB-Si-a-2	62.8	1-NO_2-3-NH_2-MDA	209.3
TB-Si-c	214.5	2-OH-benzaldehyde	85.5

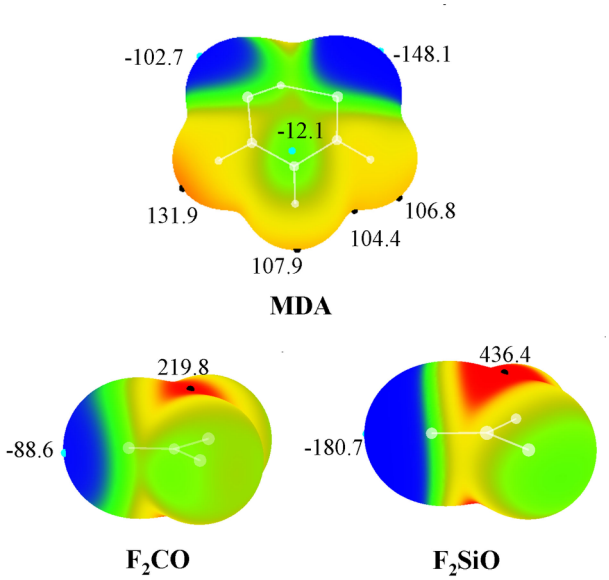

Figure 1 MEP maps of MDA and F_2TO, Color ranges are: red, greater than 131.3; yellow, between 52.5 and 0; green, between 0 and -52.5; blue, less than 52.5. All quantities are in kJ/mol.

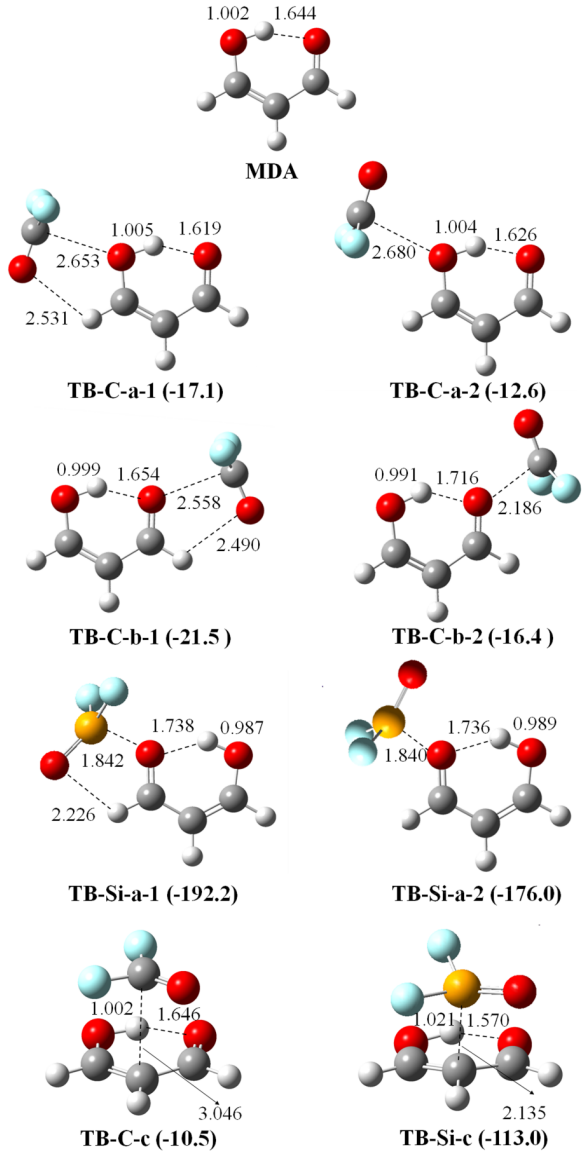

Figure 2 Structures of MDA and its complexes with F_2TO. Distances are in Å and interaction energies are in kJ/mol

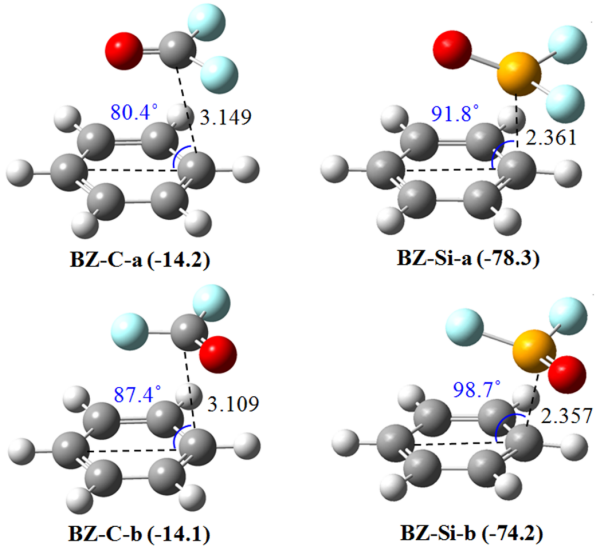

Figure 3 Structures of π-π tetrel-bonded complexes of benzene and F_2TO. Distances are in Å and interaction energies are in kJ/mol

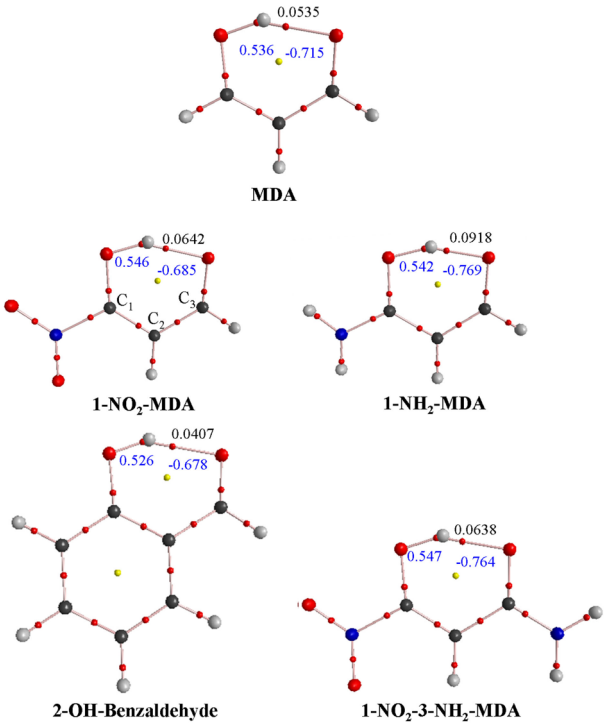

Figure 4 AIM diagrams of MDA and its derivatives. Electron densities are given in black numbers (au) and charges are in blue numbers (e)

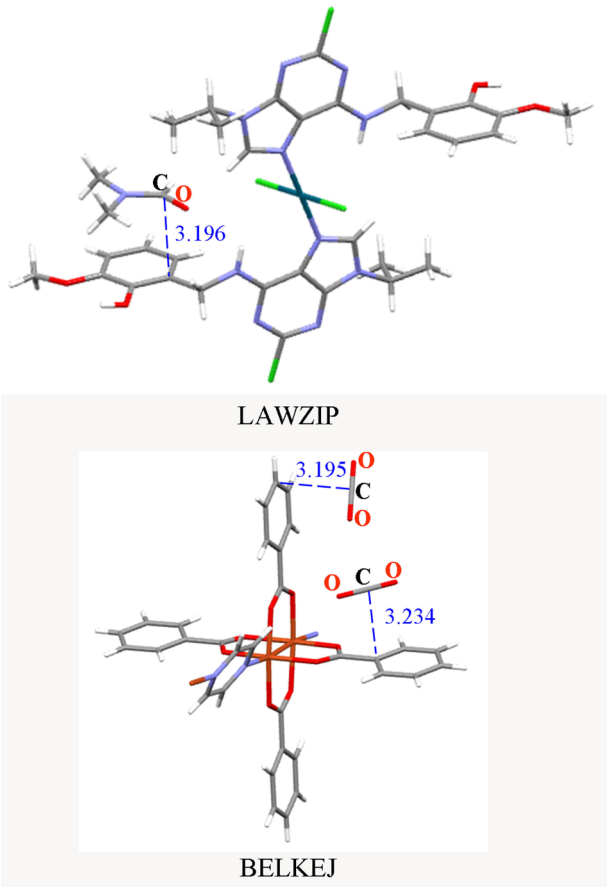

Figure 5 Crystal structures with π···π interactions between two C atoms. Distances are in angstrom.

Table of Contents Entry

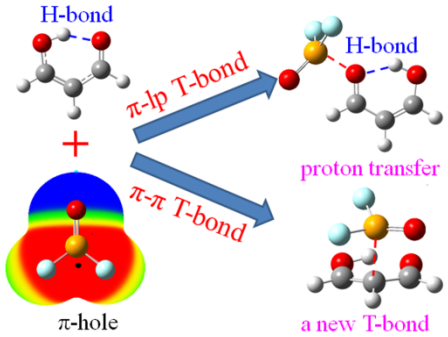

Both the hydroxyl and carbonyl groups of malonaldehyde (MDA) can form a π-tetrel bond with F_2TO (T=C and Si). F_2SiO engages in a much stronger π-tetrel bond than does F_2CO, reaching up to nearly 200 kJ/mol, and it can causes an intramoleclar proton transfer if it binds with the carbonyl group. A new sort of π-π tetrel bond occurs when the π-hole on the T atom of F_2TO approaches the middle carbon atom of MDA from above.